STEM CELLS AND DEVELOPMENT
Volume 23, Number 8, 2014

DOI: 10.1089/scd.2013.0426

Graft of a Tissue-Engineered Neural Scaffold Serves as a Promising Strategy to Restore Myelination after Rat Spinal Cord Transection

Bi-Qin Lai,[1] Jun-Mei Wang,[2] Eng-Ang Ling,[3] Jin-Lang Wu,[4] and Yuan-Shan Zeng[1,2,5]

Remyelination remains a challenging issue in spinal cord injury (SCI). In the present study, we cocultured Schwann cells (SCs) and neural stem cells (NSCs) with overexpression of neurotrophin-3 (NT-3) and its high affinity receptor tyrosine kinase receptor type 3 (TrkC), respectively, in a gelatin sponge (GS) scaffold. This was aimed to generate a tissue-engineered neural scaffold and to investigate whether it could enhance myelination after a complete T10 spinal cord transection in adult rats. Indeed, many NT-3 overexpressing SCs (NT-3-SCs) in the GS scaffold assumed the formation of myelin. More strikingly, a higher incidence of NSCs overexpressing TrkC differentiating toward myelinating cells was induced by NT-3-SCs. By transmission electron microscopy, the myelin sheath showed distinct multilayered lamellae formed by the seeded cells. Eighth week after the scaffold was transplanted, some myelin basic protein (MBP)-positive processes were observed within the transplantation area. Remarkably, certain segments of myelin derived from NSC-derived myelinating cells and NT-3-SCs were found to ensheath axons. In conclusion, we show here that transplantation of the GS scaffold promotes exogenous NSC-derived myelinating cells and SCs to form myelins in the injury/transplantation area of spinal cord. These findings thus provide a neurohistological basis for the future application or transplantation using GS neural scaffold to repair SCI.

Introduction

Spinal cord injury (SCI) is a highly prevalent medical problem. At present, there are no effective regimens that can significantly restore the function for patients with spinal cord transection [1]. This is because the pathophysiological processes in SCI are multifactorial, involving blood vessel rupture, ischemia, and edema. This together with the formation of free radicals in acute phase was followed by axonal degeneration, loss of neural cells, demyelination, and formation of cavities in the injured site [2]. For decades, experimental strategies in SCI have been focused largely on promoting axonal regeneration [3,4]. However, regeneration of axons without proper remyelination may limit functional recovery [5]. Demyelination is a hallmark feature of SCI and is an important contributor to functional loss in many disorders in the central nervous system (CNS) [6,7]. Hence, targeting remyelination is deemed to be an important therapeutic strategy for the restoration of function after SCI. On the other hand, in a complete or more severe SCI, it has become clear that there is no single ''magic bullet'' that allows concurrent remyelination, neuronal survival, and axonal regeneration [8]. In this connection, the design of a tissue-engineered neural network, with the core concept of tissue engineering consisting of cells, bioactive molecules, and scaffolds, as well as their mutual interactions seems promising [9,10]. With the optimal combination of three elements mentioned above, tissue engineering approach is expected to bridge the cavities as well as to promote the remyelination and regeneration of axons in the injured area.

One common strategy adopted by many authors to repair SCI is transplantation of neural stem cells (NSCs) [11], which have the capacity to differentiate into neurons and oligodendrocytes. However, grafted NSCs tend to differentiate into astrocytes in the lesion site [12]. Therefore, it is necessary to search for strategies to harness the therapeutic potential of NSCs in bridging lesion gap of SCI. One ideal counterstrategy would be to genetically strengthen the capacities of viability and lineage differentiation of NSCs into neurons and oligodendrocytes [13,14].

Schwann cells (SCs) secrete a plethora of trophic factors, such as nerve growth factor (NGF), brain-derived neurotrophic

[1]Key Laboratory for Stem Cells and Tissue Engineering, Ministry of Education, Sun Yat-sen University, Guangzhou, China.
[2]Department of Histology and Embryology, Zhongshan School of Medicine, Sun Yat-sen University, Guangzhou, China.
[3]Department of Anatomy, Yong Loo Lin School of Medicine, National University of Singapore, Singapore, Singapore.
[4]Department of Electron Microscope, Zhongshan School of Medicine, Sun Yat-sen University, Guangzhou, China.
[5]Institute of Spinal Cord Injury, Sun Yat-sen University, Guangzhou, China.

factor (BDNF), ciliary neurotrophic factor (CNTF), and basic fibroblast growth factor (bFGF), as well as promote extracellular matrix (ECM) and adhesion molecules [15], which have beneficial effects in supporting the function and the well-being of neurons and oligodendroglia [14]. Transplantation of SCs facilitates remyelination and axonal regeneration in the animal model of SCI [15]. However, secretion of neurotrophic factors (NTFs) by SCs is inadequate, and the capability of transplanted SCs alone to promote axonal remyelination and regeneration in the injured adult rat spinal cord is insufficient [16]. Hence, SC-based therapy could benefit from additional combinational strategies to enhance its repair potential [17]. Modifying SCs to express factors enhancing nerve regeneration and remyelination could be one strategy to improve their capacity to repair the injured CNS.

In cell transplantation therapy for SCI, attempts have been made to regulate cell fate differentiation. For this purpose, NTFs were applied to different cell types [8]. Neurotrophin-3 (NT-3) is one of the best-characterized NTFs, which interacts with its preferential receptor tyrosine kinase receptor type 3 (TrkC). NT-3 induces differentiation and myelination of oligodendrocyte progenitor cells in vitro and in vivo [18,19]. More interestingly, transplantation of NT-3 overexpressing SCs in SCI promoted the survival and differentiation of transplanted NSCs overexpressing TrkC and increased axon growth and myelination, leading to the recovery of hind limb locomotion [15].

However, the effectiveness of NTFs and/or cells transplantation in the SCI is limited, particularly when the descending and ascending nerve pathways are separated by a large gap. To circumvent this problem, tissue compatible polymers have been used [20,21]. Gelatin sponge (GS) as engineered biomaterials provides an ideal platform to deliver therapeutic cells and/or neurotrophic molecules. Sheet-like structures with large surface areas have been shown to provide a successful seal of adhered cells. The niches are believed to have profound effect on lineage specification of NSCs, which tend to differentiate into neural cells [10]. In SCI animal model, three-dimensional (3D) GS appeared to provide guidance for regenerating axons, facilitate remyelination, and prevent the infiltration of scar tissue and cyst formation [10,15].

Numerous studies have indicated that the administration of NSCs, SCs, NTFs, or tissue compatible polymers separately can yield but limited restorative benefits for SCI [8,12,20]. In this connection, engineered neural scaffold can be optimized to serve as a stratum or delivery platform taking advantage of all these treatments above. Indeed, we recently reported that coculture NT-3 gene modified SCs and TrkC gene modified NSCs in 3D SG scaffold can form a tissue-engineered neural network scaffold for structural repair and functional recovery of SCI [10]. Compared with other experiments whereby stem cells and engineered biomaterials were transplanted immediately after surgery of spinal cord, the preconstructed engineered neural scaffold with functional NSC-derived neurons and myelinating cells, and the neural network thus formed, may effectively restore the neural connectivity after spinal cord transection [10].

By interaction of SCs, NT-3/TrkC signal transduction and microenvironment of 3D GS scaffolds, NSCs in the engineered neural scaffold can be effectively induced to differentiate into neurons [67.84% ± 8.83% of neurofilament (NF)-positive cells], and to a smaller extent into oligodendrocytes [12.98% ± 5.33% of myelin basic protein (MBP)-positive cells] [10]. Here, we explored whether the tissue-engineered neural network scaffold would optimize NSC- and SC-derived myelinating cells to form myelins in vitro. In addition, and more importantly, we sought to find out if the neural network scaffold would support myelination at the lesion gap following spinal cord transection.

Materials and Methods

Preparation of NSCs and SCs

NSCs were isolated as previously described [13], from green fluorescent protein (GFP) transgenic Sprague–Dawley (SD) rats (Osaka University, Osaka, Japan). Briefly, rats (1–3 days old) were deeply anesthetized and decapitated. The whole hippocampus was then dissected and dissociated from which NSCs were derived. Culture medium containing Dulbecco's modified Eagle's medium (DMEM)/F12 (1:1; Gibco), B27 supplement (2 mL/100 mL; Gibco), and bFGF (20 ng/mL; Sigma) was used. To obtain SCs, SD postnatal rats (5–6 days old) were used. SCs were also obtained from GFP transgenic SD rats. Both the sciatic nerves and brachial plexuses were dissected. The epineurium and connective tissue were removed under a dissecting microscope. All nerves were cut into small pieces (< 2 mm) and dissociated with 0.16% collagenase (Sigma). Culture medium contained DMEM/F12 (1:1; Gibco), 10% fetal calf serum, 2 μM forskolin (Sigma), and 20 μg/mL bovine pituitary extract (Sigma). The cells were passaged when 90% confluence was reached and were purified by differential adhesion and differential digestion techniques [21].

Transfection and seeding of NSCs and SCs in GS scaffold

Recombinant adenoviral (Ad) vectors (Ad-TrkC and Ad-NT-3) were produced as described in our previous study [13]. Neurospheres were infected with Ad-TrkC. SCs were infected with Ad-NT-3. Five experimental groups were established: the NSCs, SCs + NSCs, SCs + TrkC-NSCs (SCs + T-NSCs), NT-3-SCs + NSCs (N-SCs + NSCs), and NT-3-SCs + TrkC-NSCs (N-SCs + T-NSCs or tissue-engineered neural scaffold) groups. The transfection efficiency with these viral vectors has been well documented previously by us [13,21]. Three-dimensional GS scaffolds were prepared as previously described [22]. A total of 5×10^5 cells (NSCs and SCs were mixed in 1:1 ratio) in 10 μL culture medium were seeded to each scaffold. The scaffolds were incubated for 14 days.

Cell survival and viability within GS scaffolds

Cell distribution and survival were evaluated by Hoechst33342-PI staining. The central and peripheral parts of the scaffolds were selected for study ($n = 3$ in each group). (The 1st to the 5th sections obtained were regarded as peripheral, while the 46th to the 50th sections as central). On the 14th day, 10 μg/mL Hoechst33342 and 2 μg/mL propidium iodide (PI, a membrane-impermeant DNA marker) were added. Peripheral and central sections were selected and examined. Hoechst33342 stains live cells (blue) and PI stains only dead cells (red). The death rate was calculated by

determining the percentage of dead cells (red cells) over the total cell number (blue nuclei). At least five areas (including four corners and one center) were imaged and counted for each section. Cell viability was evaluated by 3-(4,5-dimethylthiazol-2-yl)-2,5-diphenyltetrazolium bromide (MTT) assay as described previously [23] at 2, 7, and 14 days after seeding cells. The background absorption was subtracted after measuring the average OD of plain scaffolds without cells.

Spinal cord transection and transplantation

Adult female SD rats (220–250 g, supplied by the Experimental Animal Center of the Sun Yat-sen University) were used for spinal cord transection. Three days before the surgery, the rats were given cyclosporine A subcutaneous injection at the belly. All rats subjected to SCI were deeply anesthetized with 1% sodium pentobarbital (40 mg/kg, i.p.) to minimize suffering. Following laminectomy at the T9 vertebral level, a 2-mm segment of spinal cord with associated spinal roots was completely removed at the T10 spinal cord level. After hemostasis was achieved, the NT-3-SCs + TrkC-NSCs or tissue-engineered neural scaffolds (the N-SCs + T-NSCs group), GFP-NT-3-SCs + NSCs scaffolds (the GFP-NT-3-SCs group), and GS scaffolds (2-mm-long, 3-mm-diameter, the control group) were used to fill up the lesion gap, and the muscles and skin were sutured separately. After the surgical incisions were closed up, the rats received intensive postoperation care, including intramuscular injection of penicillin (50,000 U/kg/d) for 3 days and manual emiction twice daily till their automatic micturition function reestablished. Cyclosporine A was administrated once every day for 2 months. All experimental protocols and animal handling procedures were approved by the Animal Care and Use Committee of the Sun Yat-sen University and were consistent with the National Institutes of Health Guide for the Care and Use of Laboratory Animals.

Immunofluorescence staining

Specific proteins were determined using immunofluorescence staining as described in our previous studies [13,21]. Briefly, tissue sections of 25 μm thickness were cut using a cryostat. The sections were incubated with primary antibodies mixed in 0.3% Triton X-100 overnight at 4°C, followed by incubation with secondary antibodies. The slides were then examined under a fluorescence microscope. A summary of antibodies used is provided in Table 1.

Morphological quantification

For in vitro quantification of immunopositive cells, one in every 10 of the whole series of sections from each scaffold was selected ($n = 5$ in each group). After immunostained with the respective markers, five areas (0.7×0.5 mm, including four corners and one center) for each of the sections were chosen. The percentage of adenomatous polyposis coli (APC)-positive cells was calculated by counting the total number of immunopositive cells. The numerical value obtained was then divided by the total number of GFP-positive cells.

For in vivo, selected regions, 300 μm rostral to the injury/transplantation area, at the injury/transplantation area, and 300 μm caudal to the injury/transplantation area, were detected. One in every five sections from each animal was processed; a total of four sections per rat were analyzed ($n = 3$ in each group). Four 0.7×0.5 mm areas for each of the sections cut through the rostral, central, or caudal to the injury/transplantation area were chosen. The percentage of MBP-positive cells was calculated by counting the total number of

Table 1. Primary and Secondary Antibodies Used

Antibodies	*Species*	*Type*	*Dilution*	*Source*
NF 200	Mouse	Monoclonal IgG	1:1,000	Sigma (St. Louis, MO)
NF 200	Rabbit	Polyclonal IgG	1:400	Merck Millipore (Billerica, MA)
Postsynaptic density protein 95	Rabbit	Polyclonal IgG	1:800	Abcam (London, United Kingdom)
GFP	Rabbit	Polyclonal IgG	1:500	Merck Millipore (Billerica, MA)
Adenomatous polyposis coli	Rabbit	Polyclonal IgG	1:1,000	Sigma (St. Louis, MO)
Microtubule-associated protein 2	Mouse	Monoclonal IgG	1:1,000	Sigma (St. Louis, MO)
Choline acetyltransferase	Rabbit	Polyclonal IgG	1:800	Merck Millipore (Billerica, MA)
Glutamate	Rabbit	Polyclonal IgG	1:500	Boster (Wuhan, China)
Synaptophysin	Mouse	Monoclonal IgG	1:200	Sigma (St. Louis, MO)
γ-Aminobutyric acid	Rabbit	Polyclonal IgG	1:500	Boster (Wuhan, China)
TrkC	Mouse	Monoclonal IgG	1:300	R&D System (Minneapolis, MN)
NT-3	Rabbit	Polyclonal IgG	1:300	Santa Cruz Biotechnology (Santa Cruz, CA)
MBP	Rabbit	Polyclonal IgG	1:400	Merck Millipore (Billerica, MA)
Nestin	Rabbit	Polyclonal IgG	1:1,000	Sigma (St. Louis, MO)
S-100	Rabbit	Polyclonal IgG	1:500	Boster (Wuhan, China)
Cy3-conjugated anti-rabbit secondary antibody	Goat	Polyclonal IgG	1:300	Jackson ImmunoResearch, (West Grove, IA)
Alexa 647-conjugated anti-rabbit secondary antibody	Goat	Polyclonal IgG	1:500	Jackson ImmunoResearch, (West Grove, IA)
Cy3-conjugated anti-mouse secondary antibody	Goat	Polyclonal IgG	1:300	Jackson ImmunoResearch, (West Grove, IA)
AMCA-conjugated anti-rabbit secondary antibody	Goat	Polyclonal IgG	1:200	Jackson ImmunoResearch, (West Grove, IA)

AMCA, aminomethylcoumarin acetate; GFP, green fluorescent protein; MBP, myelin basic protein; NF, neurofilament; TrkC, tyrosine kinase receptor type 3.

immunopositive cells. The numerical value obtained was then divided by the total number of GFP-positive cells.

Ultrastructural observations

For scanning electron microscopy (SEM), scaffolds with cells were first washed 3 times with phosphate-buffered saline (PBS), fixed in 2.5% glutaraldehyde for 90 min, dehydrated with a series of graded ethanol, and then freeze-dried for 2 days. The dried samples were coated with gold and examined under a scanning electron microscope (Philips XL30 FEG). For transmission electron microscope (TEM), scaffolds were fixed with 2.5% glutaraldehyde at 4°C for 1 h and osmicated with 1% osmic acid for 1 h. Scaffolds were dehydrated through graded ethanol and embedded in Epon overnight, followed by polymerization at 60°C for 48 h. Semithin sections were cut on a Leica RM2065 microtome and mounted on glass slides. They were then stained with toluidine blue (5%, in a borax solution) and mounted using neutral balsam. Ultrathin sections were cut, double stained with uranyl acetate and lead citrate, and examined under an electron microscope (Philips CM 10).

For immunoelectron microscopy (IEM), rats were transcardially perfused with 0.1 M of sodium phosphate buffer containing 187.5 U/100 mL of heparin, followed by perfusion with 4% paraformaldehyde, 0.1% glutaraldehyde, and 15% saturated picric acid. Dissected spinal cord was postfixed overnight at 4°C in fresh fixative and subsequently cut into 50 μm sagittal sections on a vibratome. To improve the penetration of antibodies, vibratome sections were transferred into cryprotectant solution containing 25% sucrose and 10% glycerol in 0.1 M PBS overnight at 4°C, followed by a quick freeze-thaw in liquid nitrogen three times. After washing with PBS, the sections were treated for 1 h with 20% goat serum (Tris buffer, pH 7.4) to block nonspecific binding of the antibody. Sections were first incubated with primary antibodies (rabbit anti-GFP) in 2% normal goat serum solution at 4°C for 24 h, then incubated with secondary antibodies (goat anti-rabbit IgG nanogold®) overnight at 4°C, and postfixed in 1% glutaraldehyde for 10 min. The sections were detected by the SABC-DAB Kit and silver enhanced with the HQ silver Kit (NanoProbe 2012; Yaphank), osmicated, dehydrated, and embedded in Epon. Epon blocks were sectioned and examined under the electron microscope (Philips CM 10).

Statistical analysis

All statistical analyses were performed using the statistical software SPSS13.0. Data were reported as means ± standard deviations. When three sets of data were compared, one-way ANOVA with a LSD-*t* (equal variance assumed) or Dunnett's T3 (equal variance not assumed) was performed. A statistically significant difference was accepted at $P < 0.05$.

Results

Isolation and culture of NSCs and SCs

The majority of cells within the GFP-neurospheres were Nestin positive (Fig. 1A). At the second passage, S-100 immunofluorescence staining confirmed that the bipolar shaped positive cells were SCs (Fig. 1B).

Expression of TrkC gene in NSCs and NT-3 gene in SCs

Expression of TrkC in GFP cells infected by Ad-TrkC (MOI = 150) was detected by immunofluorescence in coculture within the GS scaffold at 14 days. About 90% of GFP cells were TrkC positive (Fig. 1C). GFP-negative SCs were infected by Ad-NT-3 (MOI = 200). There were large numbers of NT-3 overexpressing SCs around the GFP-positive cells (Fig. 1D).

Features of the cocultured cells in GS scaffold

Some myelin-like structures were observed in the semithin sections with toluidine blue staining (Fig. 2A). By TEM, the myelin sheath showed distinct multilayered lamellae presumably formed by the seeded cells (Fig. 2B). MBP, formed by GFP-negative SCs, was observed within 3D GS scaffold. Moreover, NF-positive fibers from GFP-positive NSC-derived neurons were ensheathed by MBP-positive myelin sheath (Fig. 2C). On the surface of GS, as observed by the SEM, frequent cell contacts were found between long processes of different cells, including SC-like cells (Fig. 2D, arrowhead) and neuron-like cells (Fig. 2D, arrow). Taken together, these findings suggest that GS scaffold provides an environment conducive for the adherence, extension of processes, differentiation, and myelination of seeded cells.

Survival and viability of cells in GS scaffold

To determine cell survival, cells seeded into the scaffold were cultured for 14 days and stained with Hoechst33342 and PI. Sections from the central and peripheral parts of the scaffold were selected. All cells nuclei (blue) were labeled by Hoechst33342. Dead cells (red) were marked by PI (Fig. 3A–J). The percentages of dead cells were not significantly different ($P > 0.05$, $n = 3$) between the peripheral and central sections in all experimental groups (Fig. 3K). When comparison was made between different experimental groups, the NSCs group showed significantly higher death percentage than other groups ($P < 0.05$, $n = 3$, Fig. 3K). Cell viability was determined by MTT chromometry assay. The cell viability of each group showed no statistical difference at day 1, 7, and 14 ($P > 0.05$, $n = 3$, Fig. 3L). When comparison was made between different experimental groups, cell viability of the N-SCs + NSCs and N-SCs + T-NSCs groups at day 1, the N-SCs + T-NSCs group at day 7, and the SCs + NSCs, N-SCs + NSCs and N-SCs + T-NSCs groups at day 14 was significantly higher than that of other groups ($P < 0.05$, $n = 3$, Fig. 3L). The results suggest that NT-3 may promote cell survival and viability in GS scaffold via TrkC; furthermore, the presence of SCs helped with this.

Oligodendrocyte differentiation of NSCs in GS scaffold

Fourteen days after coculture with SCs in GS scaffolds, NSCs were analyzed for their differentiation into

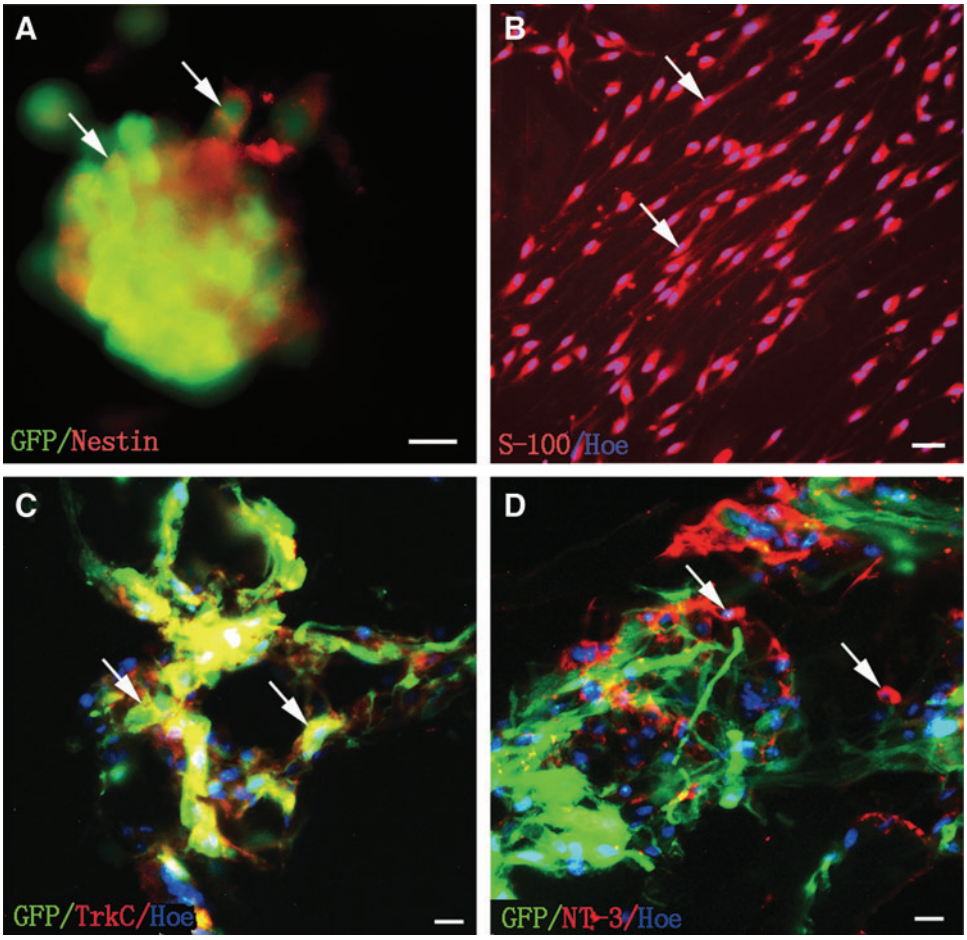

FIG. 1. Identification, gene transfection of cocultured NSCs, and SCs in the GS scaffolds. **(A)** NSCs of GFP transgene rat in vitro were labeled by Nestin (*arrows*). **(B)** SCs (*arrows*) were labeled by S-100 and Hochest33342. **(C, D)** TrkC-NSCs and NT-3-SCs were cocultured in 3D GS scaffold. **(C)** NSCs infected with Ad-TrkC emitted TrkC immunofluorescence (*arrows*). **(D)** SCs infected with Ad-NT-3 exhibited NT-3 immunofluorescence (*arrows*). Scale bars = 20 μm in **(A)**, **(C),** and **(D)**; 30 μm in **(B)**. 3D, three dimensional; GFP, green fluorescent protein; GS, gelatin sponge; NSCs, neural stem cells; NT-3, neurotrophin-3; SCs, Schwann cells; TrkC, tyrosine kinase receptor type 3.

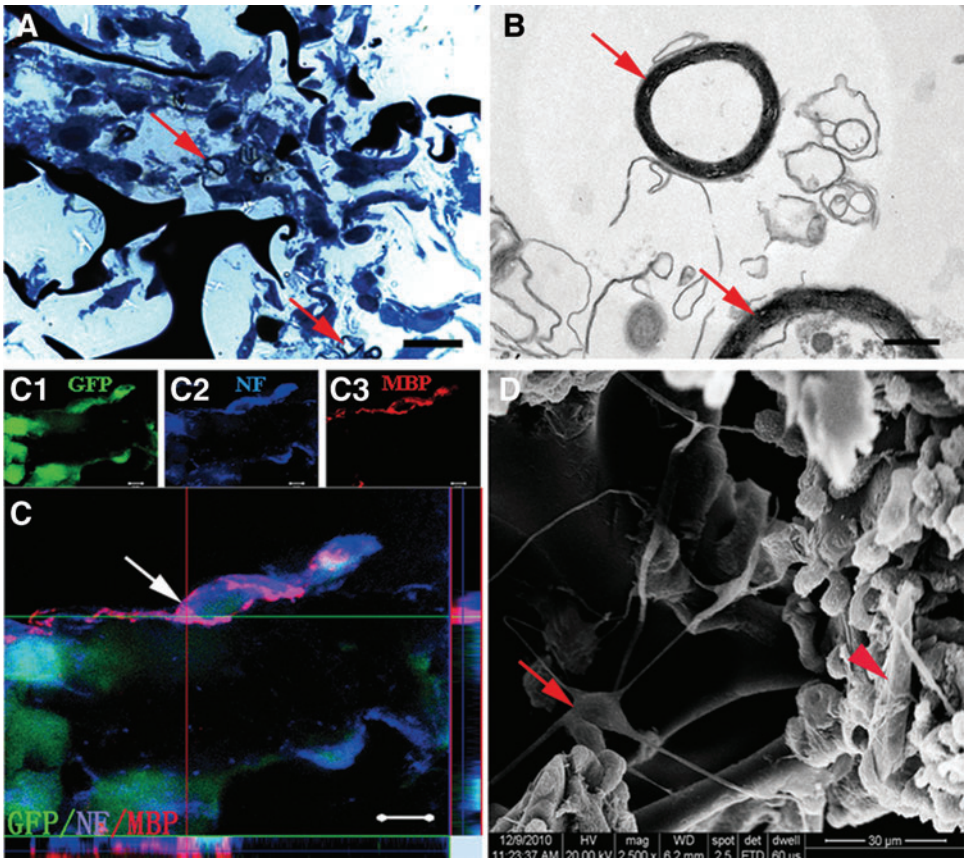

FIG. 2. Cell features and formation of myelin sheath in the GS scaffolds. **(A)** Showing a semithin section stained by toluidine blue. *Arrows* indicate myelin-like structure. **(B)** Transmission electron microscope shows two myelin-like structures (*arrows*). **(C)** A merge image of **(C1–C3)**; Note that a GFP-positive NSC-derived neuron **(C1)**, which is also NF positive **(C2)**, appears to be wrapped by MBP-positive myelin **(C3)**. The ortho section indicates MBP-positive myelin derived from GFP-negative cell. **(D)** Scanning electron microscopy shows that a multipolar cell (a neuron-like cell, *arrow*) on the surface of GS has thin and long processes. Some of these processes appear to make contacts with the cell body or processes of neighboring cells. *Arrowhead* indicates an SC-like cell. Scale bars = 20 μm in **(A)**; 0.5 μm in **(B)**; 5 μm in **(C)**; 30 μm in **(D)**. MBP, myelin basic protein.

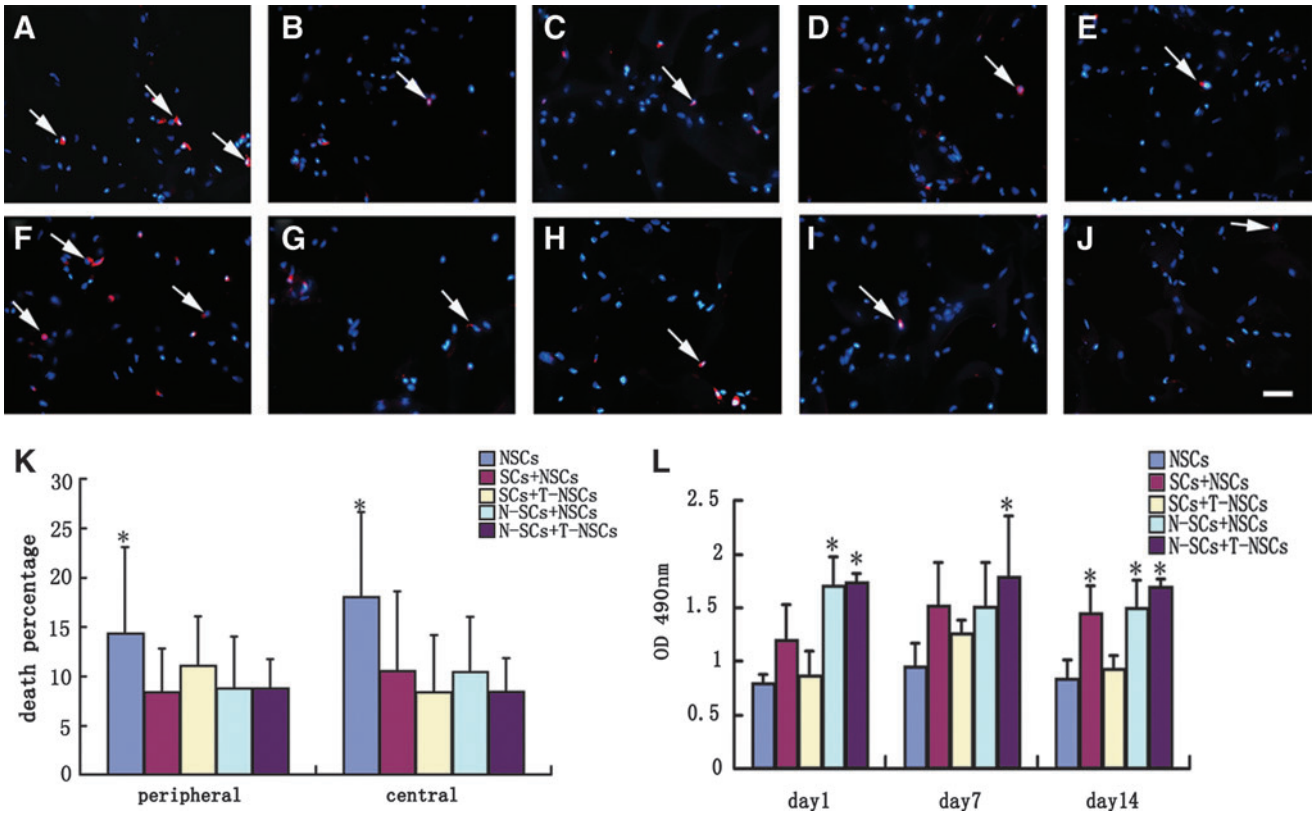

FIG. 3. Survival and viability of cells in 3D GS scaffolds. Cells in the peripheral **(A–E)** and central **(F–J)** parts of 3D GS scaffold were stained with PI and Hoechst33342. Dead cells (*arrows*) were double labeled by PI and Hoechst33342. Scale bars = 40 μm in **(A–J)**. **(K)** Bar chart showing the percentage of dead cells in the peripheral and central parts of 3D GS scaffolds. Statistical difference ($*P < 0.05$) in percentage of dead cells of the NSCs group, compared with other groups. Results are presented as mean ± standard deviation. One-way ANOVA with an LSD-t was performed. **(L)** Bar chart showing the cell viability of the scaffolds following MTT test. *Asterisks* indicate that the cells viability of the N-SCs + NSCs (day 1), N-SCs + T-NSCs (day 1), N-SCs + T-NSCs (day 7), SCs + NSCs (day 14), N-SCs + NSCs (day 14), and N-SCs + T-NSCs (day 14) groups were significantly higher compared with other groups ($*P < 0.05$). Results are presented as mean ± standard deviation. One-way ANOVA with a LSD-t was performed. **(A, F)** NSCs group; **(B, G)** SCs + NSCs group; **(C, H)** SCs + T-NSCs group; **(D, I)** N-SCs + NSCs group; **(E, J)** N-SCs + T-NSCs group. PI, propidium iodide.

oligodendrocytes (APC-positive staining, Fig. 4A–E). Results of cell counting showed that the percentage of APC-positive cells (11.98% ± 4.56%) in the N-SCs + NSCs group and (12.98% ± 5.33%) in the N-SCs + T-NSCs group was more than that in the NSCs, SCs + NSCs, and SCs + T-NSCs groups (Fig. 4F).

Axonal regeneration and remyelination of transplanted cells in injured spinal cord

Eight weeks after SCI, GFP-positive cells could be observed in the entire injury/transplantation area of spinal cord as well as in the rostral injury/transplantation area (Fig. 5A). Most of the transplanted GFP-positive cells exhibited NF-positive immunostaining and extended their processes in the injury/transplantation area (Fig. 5B). Host NF-positive fibers were also found closely associated with GFP cells (Fig. 5B). MBP, a protein on the compact myelin, was observed within the injury/transplantation area. Remarkably, certain segments of NF-positive fibers from NSC-derived neurons or host neurons were ensheathed by MBP-positive myelin sheath (Fig. 5C). These results suggest that graft of the neural scaffold can create a favorable microenvironment for better cell survival and myelination in the injury/transplantation area of spinal cord.

NSC-derived neurons expressed neurotransmitters

Some GFP-positive cells grafted into the injury/transplantation area of spinal cord were capable of synthesizing neurotransmitters. The cell bodies and their processes of NSC-derived neurons (GFP-positive cells) containing glutamate and acetylcholine were observed, but not gamma-aminobutynic acid (GABA) (Fig. 6A–L). This suggests that NSC-derived neurons may transmit neural signals for neuronal communication in the injury/transplantation area of spinal cord.

Myelination of nerve fibers by NSC-derived myelinating cells and SCs

On neural scaffold transplantation, although most of the GFP-positive NSCs in the injury/transplantation area of spinal cord extended long NF-positive nerve fibers, there

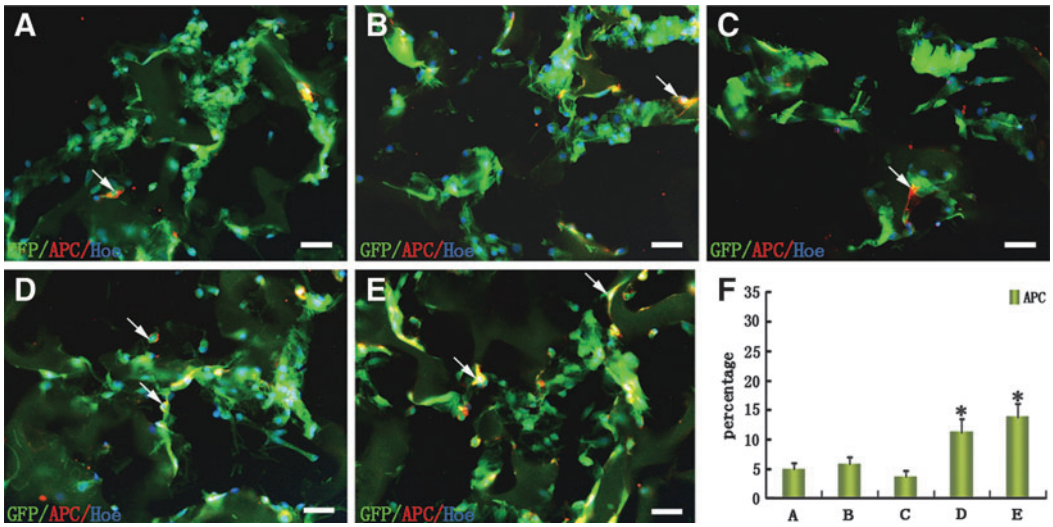

FIG. 4. Oligodendrocytic differentiation of NSCs in the GS scaffolds. **(A–E)** Cells (*arrows*) were labeled by oligodendrocytic marker (APC). **(F)** Bar chart showing the percentage of MBP-positive cells in five groups of GFP-positive cells. *Asterisks* indicate statistical significance between the N-SCs + NSCs or N-SCs + T-NSCs groups and the other (NSCs, SCs + NSCs, or SCs + T-NSCs) groups ($*P < 0.05$). Results are presented as mean ± standard deviation ($n = 5$). One-way ANOVA with a LSD-*t* was performed. Scale bars = 20 μm in **(A–E)**. **(A)** NSCs group; **(B)** SCs + NSCs group; **(C)** SCs + T-NSCs group; **(D)** N-SCs + NSCs group; **(E)** N-SCs + T-NSCs group. APC, adenomatous polyposis coli.

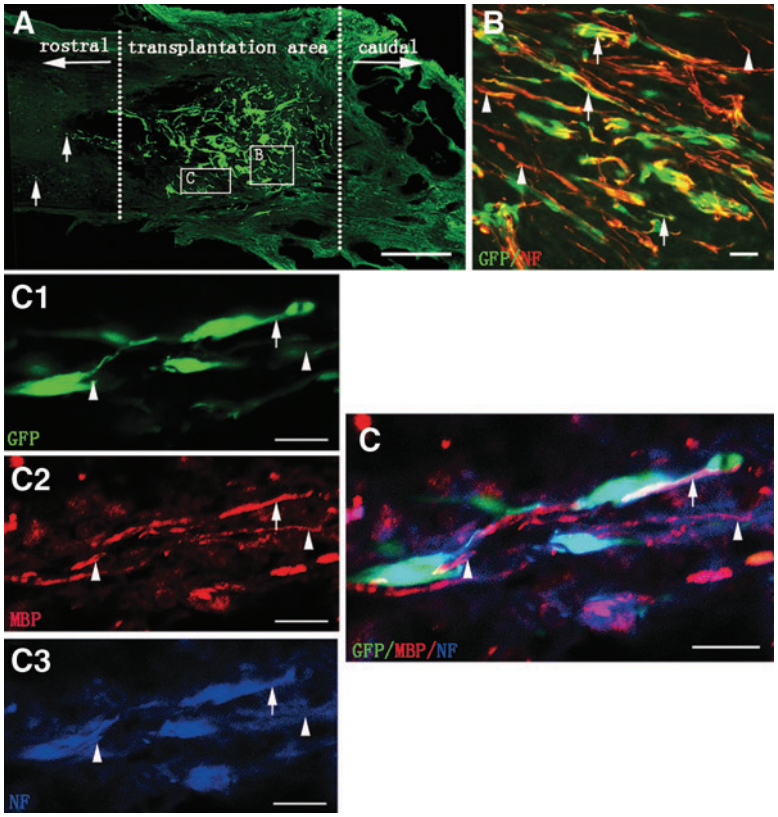

FIG. 5. Cell survival, innervation, and myelination of the tissue-engineered neural scaffold transplanted in injured spinal cord. **(A)** Showing the cell survival of transplanted scaffold at eighth week in the N-SCs + T-NSCs group in a longitudinal section of injured spinal cord. Note that GFP-positive cells (*green*) of the neural scaffold transplanted are mainly distributed in the injury/transplantation area of spinal cord. The neural scaffold appears to integrate well with host tissue. Some of the GFP-positive cells (*arrows*) have migrated farther to the rostral of the injury/transplantation area. Leading diagram **(A)** depicts the cells' sampling sites in the spinal cord. **(B)** Showing transplanted NSC-derived neurons. NF-positive neurons (GFP-positive labeling) extend their processes (*arrows*). Some NF-positive axons from host (*arrowheads*) are distributed around GFP- and NF-positive double labeling axons. **(C)** Myelination of axons in the injury/transplantation area. Axons both from host (*arrowheads* in **C3** and **C**) or NSC-derived neurons (*arrows* in **C1, C3** and **C**) undergo robust myelination (*arrows* in **C2** and **C**). GFP and NF positive double labeling cells (*arrows* in **C**) with thin axon are wrapped by MBP positive myelin sheath (*arrow* in **C2**). Scale bars = 500 μm in **(A)**; 20 μm in **(B)** and **(C)**.

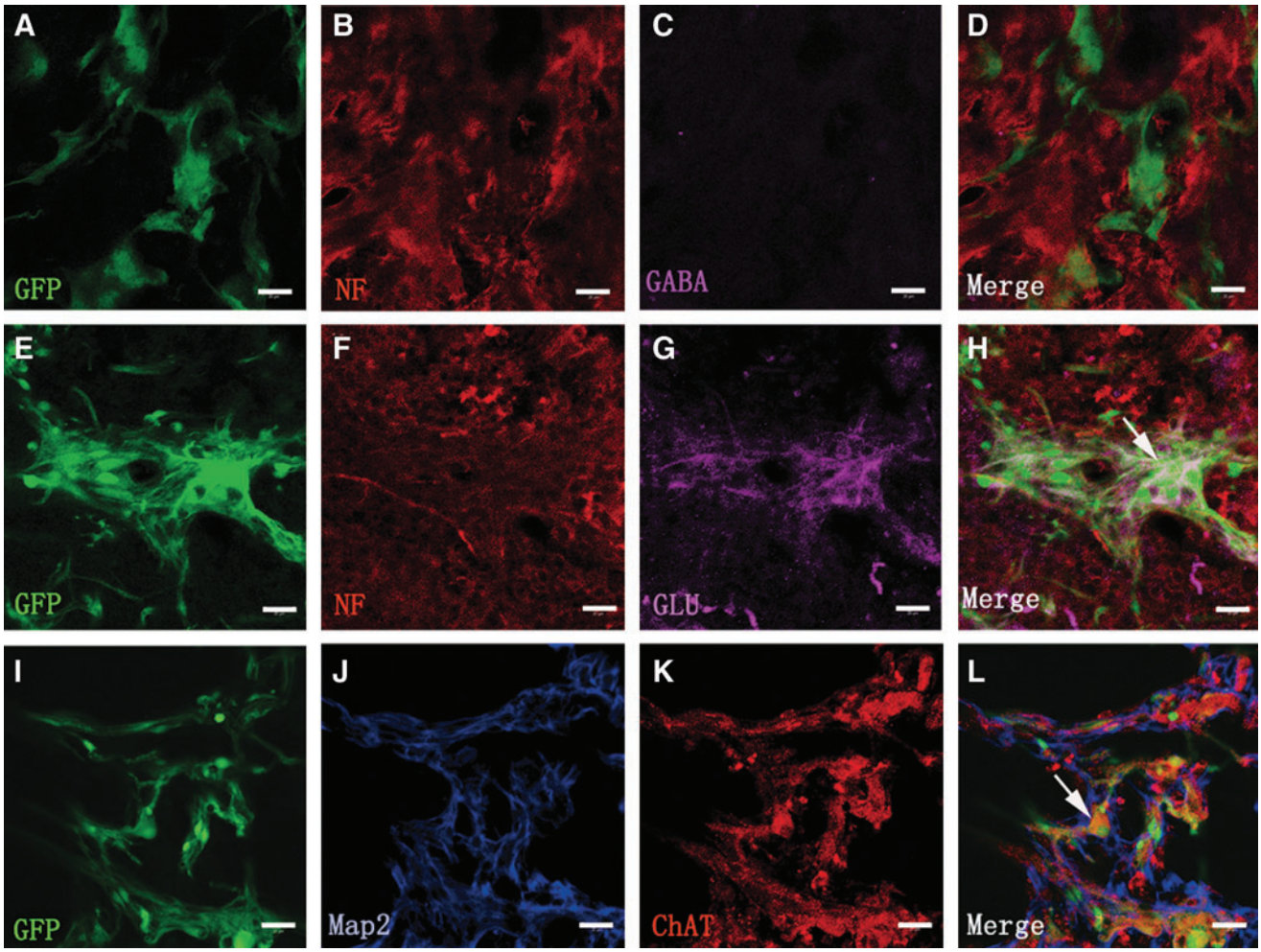

FIG. 6. Neurotransmitter expression of NSC-derived neurons. **(A–L)** Showing the NSC-derived neurons expressing neurotransmitters as assessed by immunofluorescence staining of NF/Map2 together with GABA **(D)**, glutamate (*arrow* in **H**), or ChAT (*arrow* in **L**) eighth week after transplantation. Some NSC-derived neurons maintain the expression of neuronal marker NF/Map2 and neurotransmitter glutamate **(G)** and ChAT **(K)**, but not GABA **(C)**. Scale bars = 30 μm in **(A–L)**. ChAT, choline acetyltransferase; GABA, γ-Aminobutyric acid.

were some GFP-positive NSCs differentiating into myelinating cells (the N-SCs + T-NSCs group). Some NF-positive axons appeared to be remyelinated by these NSC-derived myelinating cells (Fig. 7A–D). By IEM, GFP-positive myelinating cells lacking a layer of basal lamina formed myelin structure surrounding axons (Fig. 7E, F). We next ascertained if SCs overexpressing NT-3 (the GFP-NT-3-SCs group) would also take part in myelination after the neural scaffold transplanted into the injury/transplantation area of spinal cord. GFP-NT-3-SCs in the neural scaffold grafted were observed in the injury/transplantation area (Fig. 8A, B). Immunohistochemistry revealed robust expression of MBP in GFP-NT-3-SCs, which ensheathed NF-positive axons (Fig. 8C). These results suggest that NSC-derived myelinating cells and NT-3-SCs in the neural scaffold grafted can form myelin sheath ensheathing the regenerating axons in the injury/transplantation area of spinal cord. The high incidence of MBP-positive cells among GFP-transplanted cells also indicates that most of the NSC-derived myelinating cells and NT-3-SCs contribute to form myelin (Table 2).

Discussion

Axonal regeneration and remyelination in the injured spinal cord has been a major therapeutic challenge for years. This is particularly problematic when there is a large gap separating the injured cord between the rostral and caudal segments [15,20]. In the present study, we cocultured NT-3 gene-modified SCs with TrkC gene-modified NSCs in 3D GS scaffolds to systemically investigate the remyelination potential of the tissue-engineered neural network scaffold grafted into the lesion gap of spinal cord transection. Our results suggest that the NSC-derived myelinating cells and SCs in the tissue-engineered neural network scaffold grafted can form myelin-like structure, which ensheathed the regenerating axons in the injury/transplantation area of spinal cord.

Our previous studies have shown that SCs overexpressing NT-3 induced most of NSCs overexpressing TrkC into NSC-derived neurons in vitro [10]. Through SEM, we detected a large number of cells, including SC-like cells and neuron-like cells. The present study also showed that SCs, together with those overexpressing NT-3, induced a small

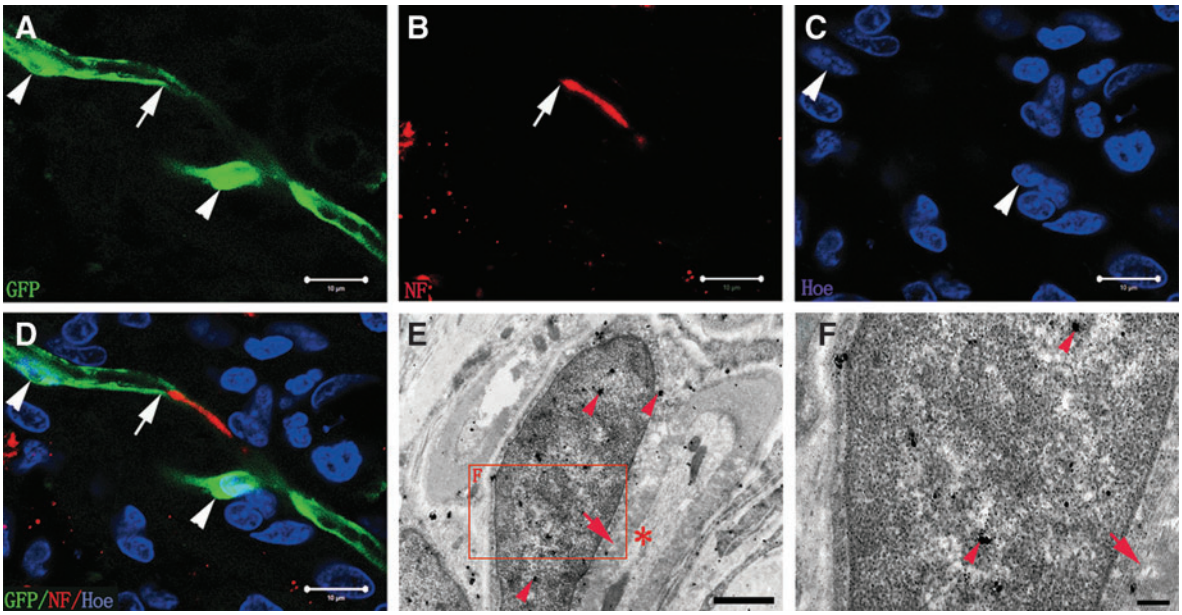

FIG. 7. Myelination of axons by NSC-derived myelinating cells (the N-SCs + T-NSCs group). **(A, B)** GFP-positive NSC-derived myelinating cell (*arrow*, **A**) appears to wrapped NF-positive axon (*arrow*, **B**). **(C)** Showing the nucleus (*arrowheads*) of NSC-derived myelinating cells. **(D)** A merge image of **(A–C)**. **(E)** To verify the identity of the myelinating cell, we performed immunological EM with GFP antibodies that were labeled by secondary antibodies conjugated with gold particles and silver-enhanced. GFP is highly concentrated in the myelinating cell (*arrowheads*), thus confirming that this cell is an NSC-derived myelinating cell. An axon (*asterisk*) is inside the myelin structure (*arrow*). **(F)** The magnified image of *boxed area* in **(E)** shows that the NSC-derived myelinating cell does not have the basal lamina. Scale bars = 10 μm in **(A–D)**; 1 μm in **(E)**; 200 nm in **(F)**.

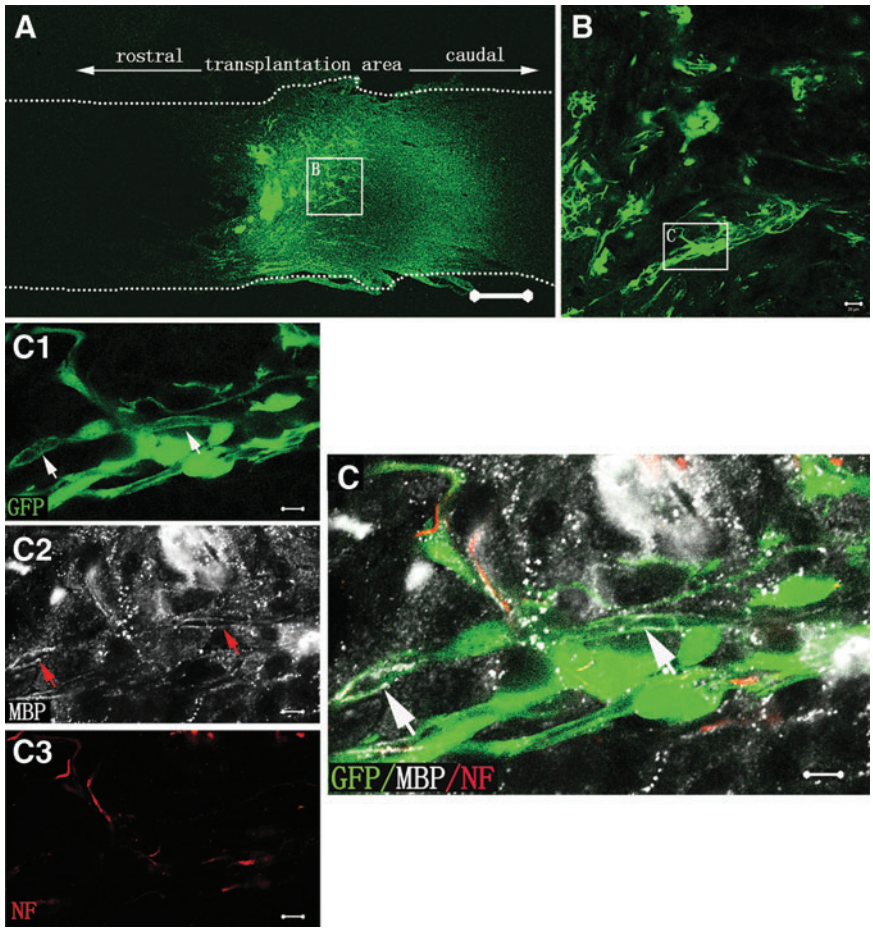

FIG. 8. Myelinating cells from exogenous SCs graft (the GFP-NT-3-SCs group). **(A)** Showing an overview of a longitudinal section of spinal cord segment containing the GFP-NT-3-SCs graft, to observe exogenous SCs and their effect on mediating myelination. **(B)** GFP-positive NT-3-SCs in the injury/transplantation area of spinal cord were detected. **(C)** A higher magnification of *boxed area* in **(B)** shows the overlaid image of GFP **(C1)**, MBP **(C2)**, and NF **(C3)** labeling objects. *Arrows* indicate some GFP-positive NT-3-SCs forming myelin-like structures, which are also MBP positive. Some NT-3-SCs contact very closely with NF-positive nerve fibers. Scale bars = 500 μm in **(A)**; 20 μm in **(B)**; 5 μm in **(C)**, **(C1–C3)**.

Table 2. Percentage (Mean ± Standard Deviation, %) of Myelin Basic Protein-Positive Cell Among Green Fluorescent Protein-Transplanted Cells In Vivo

Group	n	*MBP*
N-SCs + T-NSCs	3	9.36 ± 0.67
GFP-NT-3-SCs	3	86.27 ± 2.14

SCs, Schwann cells; NT-3, neurotrophin-3.

portion of NSCs differentiating into oligodendrocytes. This was confirmed by the intense expression of APC, an oligodendrocyte marker, notably in the N-SCs + NSCs and N-SCs + T-NSCs groups. The results are consistent with the known evidence that NT-3 promotes oligodendrocyte precursor cell (OPC) maturation and myelination [14,24]. We speculate that NT-3 may facilitate oligodendrocyte development through $p75^{NTR}$ [25]. An interesting characteristic of $p75^{NTR}$ is its high level of expression in SCs during development and remyelination paradigms [26]. That may be one of the reasons why SCs of the N-SCs + T-NSCs group in the scaffold appeared to form myelin and ensheath NF-positive fibers of NSC-derived neurons.

Much less is known, however, about the intrinsic mechanisms governing myelination. SCs overexpressing NT-3 not only provide NT-3 but also secrete many types of trophic factors, such as NGF, BDNF, CNTF, and bFGF, as well as ECM and adhesion molecules [15,21]. Cultured cells on gelatin matrix of the GS scaffold may also be an important reason since 3D scaffold is believed to better represent the microenvironment of CNS [27] to promote survival and function of neurons and to facilitate myelination than 2D culture [28]. Previous studies of methacrylate hydrogels as cell-polymer scaffolds reported only modest stem cell survival during 14-day culture in vitro [29]. Park and colleagues reported recently that viability of chondrocytes in engineered cartilage was better in the periphery than in the center in vitro [30]. In the light of the above, it is suggested that the improved survival, viability, and formation of neural network in the present study may be attributed to the use of 3D GS scaffolds and SCs overexpressing NT-3, together with NT-3/TrkC signal transduction.

All of these factors, such as NT-3/TrkC and/or NT-3/$P75^{NTR}$ signal cascade, oligodendrocytes, SCs, the nature of 3D gelatin matrix, might act together to create a favorable microenvironment, which supports myelination in the neural network scaffold. In the present neural scaffolds, the majority of NSCs became neurons, while only a small portion of them differentiated into oligodendrocytes. A striking feature in the neural scaffolds was the occurrence of numerous NSC-derived neurons forming functional synaptic contacts [10]. The neurons were admixed with NT-3 overexpressing SCs, oligodendrocytes, and formation of the myelin sheath in vitro. The present results have provided evidence supporting the use of a preconstructed neural network scaffold that has an optimal myelination potential in vitro. Unlike studies by others in which transplanted stem cells or progenitor cells were used to restore myelination [11,31,32], we have transplanted a preconstructed tissue-engineered neural scaffold to serve as potential conduits in neural repair in SCI.

In CNS, axon myelination facilitates neuronal performance by increasing the speed of neuronal conductance. Loss of oligodendrocytes and myelin results in severe functional impairment [33,34]. Some studies also support the key role of remyelination in promoting neuronal survival after adult CNS injury [35,36]. It remains to be proven whether the neural network scaffold that we created in vitro is able to encircle axons by myelin sheath and improve nerve conduction in injured spinal cord. Eight weeks after the scaffold transplantation, robust innervation and remyelination occupied the injury/transplantation area of spinal cord. Numerous NSC-derived neurons maintained the NF immunofluorescence and extended their processes as in vitro. MBP, a protein on the compact myelin, which either represents the myelin from the NSC-derived myelinating cells or from GFP-NT-3-SCs, was observed. The amount of remyelination also showed that most of the NSC-derived myelinating cells and GFP-NT-3-SCs are committed to form myelin ensheathing NF-positive fibers (Figs. 7 and 8 and Table 2). This indicates that the transplants can create a favorable microenvironment conducive for cell survival and myelination and also indicates that complex cell–cell signaling may regulate myelin formation on appropriate axons since myelination is a fine-tuning biological process that is regulated by a close coordination between oligodendrocytes/SCs and neuron/axon [36].

Electrical activity has been shown to affect the proliferation and differentiation of myelinating neuroglia, to regulate subcellular events necessary for myelin induction [37,38]. Myelin could form preferentially on electrically active axons [39]. One of the striking features in our study was the occurrence of many NSC-derived neurons as well as host regenerating axons bearing extending long processes that were encircled by myelin sheath. Together with the evidence was that NSC-derived neurons in our neural network scaffold could communicate with others via releasing neurotransmitters or producing electrical signals [10]. We conclude that myelinogenesis increases in response to electrical excitation and activity-dependent molecular cascades, then protecting the axon from damage, guiding the axon regeneration, and finally, increasing the speed of nerve impulse transmission.

For severe SCI, the effort to replace neuron loss and to promote axon regeneration is insufficient for functional recovery [2,5]. A possible reason for this may be that oligodendrocytes undergo apoptosis, and although spontaneous remyelination occurs, endogenous OPCs supply is limited and inadequate for functional improvement. NT-3 overexpressing SCs significantly improve remyelination by which NT-3 recruits OPCs [34,40]. It is suggested that SCs may play a critical role as myelinogenic cells to facilitate axon regeneration, act as a bridge, support axonal outgrowth, and finally ensheath axons to mediate functional recovery [41,42]. Based on previous reports, we hypothesized that NT-3 overexpressing SCs could promote oligodendrocyte development and maturation in the neural network scaffold grafted. Indeed, our study demonstrated that myelinating cells also serve as a guide for axon regeneration and myelination by cell–axon contact.

In summary, seeding SCs and NSCs with genetically engineered overexpression of NT-3 and its high affinity receptor TrkC, respectively, in the GS scaffold, we have constructed a tissue-engineered neural (NT-3-SCs + TrkC-NSCs) scaffold to bridge the spinal cord after T10

transection. This strategy increased NSC-derived myelinating cells differentiation and SC-based myelination, which appear to help ensheath regenerating/growing axons through remyelination in the injury/transplantation area of spinal cord. The results suggest that the integration of exogenous tissue-engineered neural network scaffold and endogenous neural network structure with good axonal remyelination may work as a relay structurally and functionally for repairing spinal cord transection. Furthermore, this model in vitro will be a useful tool to investigate precise effects of genetic modifications, in terms of cell–cell interactions, neurite outgrowth and myelination, on neurons, oligodendrocytes, and SCs.

Acknowledgment

This research was supported by the grants from the Chinese National Natural Science Foundation (no. 81330028; no. U1301223), National 863 Project (no. 2013AA020106), Foundation of the Education Ministry of China (no. 201300193035), Emphasis Foundation of Social Developmental Field of Guangdong Province (no. 2011A030300004), and Scientific Foundation of Guangzhou City (no. 2012J4100077) to Y.-S.Z.

Author Disclosure Statement

No competing financial interests exist.

References

1. Tuszynski MH and O Steward. (2012). Concepts and methods for the study of axonal regeneration in the CNS. Neuron 74:777–791.
2. Musienko P, J Heutschia, L Friedli, R van den Brand, and G Courtine. (2012). Multi-system neurorehabilitative strategies to restore motor functions following severe spinal cord injury. Exp Neurol 235:100–109.
3. Ramon-Cueto A, MI Cordero, FF Santos-Benito, and J Avila. (2000). Functional recovery of paraplegic rats and motor axon regeneration in their spinal cords by olfactory ensheathing glia. Neuron 25:425–435.
4. Abematsu M, K Tsujimura, M Yamano, M Saito, K Kohno, J Kohyama, M Namihira, S Komiya, and K Nakashima. (2010). Neurons derived from transplanted neural stem cells restore disrupted neuronal circuitry in a mouse model of spinal cord injury. J Clin Invest 120:3255–3266.
5. Lu P, A Blesch, L Graham, YZ Wang, R Samara, K Banos, V Haringer, L Havton, and N Weishaupt. (2012). Motor axonal regeneration after partial and complete spinal cord transection. J Neurosci 32:8208–8218.
6. Hu JG, L Shen, R Wang, QY Wang, C Zhang, J Xi, SF Ma, JS Zhou, and HZ Lu. (2012). Effects of Olig2-overexpressing neural stem cells and myelin basic protein-activated T cells on recovery from spinal cord injury. Neurotherapeutics 9:422–445.
7. Onifer SM, GM Smith, and K Fouad. (2011). Plasticity after spinal cord injury: relevance to recovery and approaches to facilitate it. Neurotherapeutics 8:283–293.
8. Ruff CA, JT Wilcox, and MG Fehlings. (2012). Cell-based transplantation strategies to promote plasticity following spinal cord injury. Exp Neurol 235:78–90.
9. Xiong Y, YS Zeng, CG Zeng, BL Du, LM He, DP Quan, W Zhang, JM Wang, JL Wu, et al. (2009). Synaptic transmission of neural stem cells seeded in 3-dimensional PLGA scaffolds. Biomaterials 30:3711–3722.
10. Lai BQ, JM Wang, JJ Duan, YF Chen, HY Gu, EA Ling, JL Wu, and YS Zeng. (2013). The integration of NSC-derived and host neural networks after rat spinal cord transection. Biomaterials 34:2888–2901.
11. Uchida N, K Chen, M Dohse, KD Hansen, J Dean, JR Buser, A Riddle, DJ Beardsley, and Y Wan. (2012). Human neural stem cells induce functional myelination in mice with severe dysmyelination. Stem cell 4:1–11.
12. Novikova LN, LN Novikov, and JO Kellerth. (2002). Differential effects of neurotrophins on neuronal survival and axonal regeneration after spinal cord injury in adult rats. J Comp Neurol 452:255–263.
13. Wang JM, YS Zeng, RY Liu, WL Huang, Y Xiong, YH Wang, SJ Chen, and YD Teng. (2007). Recombinant adenovirus vector-mediated functional expression of neurotropin-3 receptor (TrkC) in neural stem cells. Exp Neurol 203:123–127.
14. Xiong Y, JX Zhu, ZY Fang, CG Zeng, C Zhang, GL Qi, MH Li, W Zhang, and DP Quan. (2012). Coseeded Schwann cells myelinate neurites from differentiated neural stem cells in neurotrophin-3-loaded PLGA carriers. Int J Nanomedicine 7:1977–1989.
15. Wang JM, YS Zeng, JL Wu, Y Li, and Y D Teng. (2011). Cograft of neural stem cells and Schwann cells overexpressing TrkC and neurotrophin-3 respectively after rat spinal cord transection. Biomaterials 32:7454–7468.
16. Xu XM, A Chen, V Guenard, N Kleitman, and MB Bunge. (1997). Bridging Schwann cell transplants promote axonal regeneration from both the rostral and caudal stumps of transected adult rat spinal cord. J Neurocytol 26:1–16.
17. Lu P and MH Tuszynski. (2008). Growth factors and combinatorial therapies for CNS regeneration. Exp Neurol 209:313–320.
18. Jean I, C Lavialle, A Barthelaix-Pouplard, and C Fressinaud. (2003). Neurotrophin-3 specifically increases mature oligodendrocyte population and enhances remyelination after chemical demyelination of adult rat CNS. Brain Res 972:110–118.
19. Rubio N, R Rodriguez, and MA Arevalo. (2004). In vitro myelination by oligodendrocyte precursor cells transfected with the neurotrophin-3 gene. Glia 47:78–87.
20. Teng YD, EB Lavik, X Qu, KI Park, J Ourednik, D Zurakowski, R Langer, and EY Snyder. (2002). Functional recovery following traumatic spinal cord injury mediated by a unique polymer scaffold seeded with neural stem cells. Proc Natl Acad Sci U S A 99:3024–3029.
21. Zhang XB, YS Zeng, W Zhang, JM Wang, JL Wu, and J Li. (2007). Co-transplantation of neural stem cells and NT-3-overexpressing Schwann cells in transected spinal cord. J Neurotrauma 24:1863–1877.
22. Zeng X, YS Zeng, YH Ma, LY Lu, BL Du, W Zhang, Y Li, and WY Chan. (2011). Bone marrow mesenchymal stem cells in a three dimensional gelatin sponge scaffold attenuate inflammation, promote angiogenesis and reduce cavity formation in experimental spinal cord injury. Cell Transplant 20:1881–1899.
23. Mattii L, B Battolla, D D'Alessandro, L Trombi, S Pacini, MG Cascone, L Lazzeri, N Bernardini, A Dolfi, S Galimberti, and M Petrini. (2008). Gelatin/PLLA sponge-like scaffolds allow proliferation and osteogenic differentiation of human mesenchymal stromal cells. Macromol Biosci 8:819–826.

24. Hu X, L Jin, and L Feng. (2005). Erk1/2 but not PI3K pathway is required for neurotrophin 3-induced oligodendrocyte differentiation of post-natal neural stem cells. J Neurochem 90:1339–1347.
25. Cosgaya JM, JR Chan, and EM Shooter. (2002). The neurotrophin receptor $p75^{NTR}$ as a positive modulator of myelination. Science 298:1245–1248.
26. Heumann R, D Lindholm, C Bandtlow, M Meyer, MJ Radeke, TP Misko, E Shooter, and H Thoenen. (1987). Differential regulation of mRNA encoding nerve growth factor and its receptor in rat sciatic nerve during development, degeneration, and regeneration: role of macrophages. Proc Natl Acad Sci U S A 84:8735–8739.
27. Chan V, P Zorlutuna, JH Jeong, H Kong, and R Bashir. (2010). Three-dimensional photopatterning of hydrogels using stereolithography for long-term cell encapsulation. Lab Chip 10:2062–2070.
28. Xu T, CA Gregory, P Molnar, X Cui, S Jalota, SB Bhaduri, and T Boland. (2006). Viability and electrophysiology of neural cell structures generated by the inkjet printing method. Biomaterials 27:3580–3588.
29. Hejcl A, J Ruzicka, M Kapcalova, K Turnovcova, E Krumbholcova, M Pradny, J Michalek, J Cihlar, P Jendelova, and E Sykova. (2013). Adjusting the chemical and physical properties of hydrogels leads to improved stem cell survival and tissue ingrowth in spinal cord injury reconstruction: A comparative study of four methacrylate hydrogels. Stem Cells Dev 22:2794–2805.
30. Park K, BH Min, DK Han, and K Hasty. (2007). Quantitative analysis of temporal and spatial variations of chondrocyte behavior in engineered cartilage during long-term culture. Ann Biomed Eng 35:419–428.
31. Yang JX, ZL Jiang, DC Fitzgerald, CG Ma, S Yu, HM Li, Z Zhao, YH Li, and B Ciric. (2009). Adult neural stem cells expressing IL-10 confer potent immunomodulation and remyelination in experimental autoimmune encephalitis. J Clin Invest 119:3678–3691.
32. Taghipour Z, K Karbalaie, A Kiani, A Niapour, H Bahramian, MH Nasr-Esfahani, and H Baharvand. (2012). Transplantation of undifferentiated and induced human exfoliated deciduous teeth-derived stem cells promotes functional recovery of rat spinal cord contusion injury model. Stem Cells Dev 21:1794–1802.
33. Zhang YJ, W Zhang, CG Lin, Y Ding, SF Huang, JL Wu, Y Li, HX Dong, and YS Zeng. (2012). Neurotrophin-3 gene modified mesenchymal stem cells promote remyelination and functional recovery in the demyelinated spinal cord of rats. J Neurol Sci 313:64–74.
34. Huang SF, Y Ding, JW Ruan, W Zhang, JL Wu, B He, YJ Zhang, Y Li, and YS Zeng. (2011). An experimental electro-acupuncture study in treatment of the rat demyelinated spinal cord injury induced by ethidium bromide. Neurosci Res 70:294–304
35. Griffiths I, M Klugmann, T Anderson, D Yool, C Thomson, MH Schwab, A Schneider, F Zimmermann, and M McCulloch. (1998). Axonal swellings and degeneration in mice lacking the major proteolipid of myelin. Science 280:1610–1613.
36. Nave KA. (2010). Myelination and support of axonal integrity by glia. Nature 468:244–252.
37. Demerens C, B Stankoff, M Logak, P Anglade, B Allinquant, F Couraud, B Zalc, C Lubetzki. (1996). Induction of myelination in the central nervous system by electrical activity. Proc Natl Acad Sci U S A 93:9887–9892.
38. Stevens B and RD Fields. (2000). Response of Schwann cells to action potentials in development. Science 287: 2267–2271.
39. Wake H, PR Lee, and RD Fields. (2011). Control of local protein synthesis and initial events in myelination by action potentials. Science 333:1647–1651.
40. Kusano K, M Enomoto, T Hirai, P Tsoulfas, S Sotome, K Shinomiya, and A Okawa. (2010). Transplanted neural progenitor cells expressing mutant NT3 promote myelination and partial hindlimb recovery in the chronic phase after spinal cord injury. Biochem Biophys Res Commun 393: 812–817.
41. Salzer JL. (2012). Axonal regulation of Schwann cell ensheathment and myelination. J Peripher Nerv Syst 17: 14–19.
42. Lavdas AA, J Chen, F Papastefanaki, S Chen, M Schachner, R Matsas, and D Thomaidou. (2010). Schwann cells engineered to express the cell adhesion molecule L1 accelerate myelination and motor recovery after spinal cord injury. Exp Neurol 221:206–216.

Address correspondence to:
Yuan-Shan Zeng
Department of Histology and Embryology
Zhongshan School of Medicine
Sun Yat-sen University
74# Zhongshan 2nd Road
Guangzhou 510080
China

E-mail: zengysh@mail.sysu.edu.cn

Received for publication September 6, 2013
Accepted after revision December 5, 2013
Prepublished on Liebert Instant Online December 10, 2013